

DOPPLERFREE SPECTROSCOPY OF RUBIDIUM

Physikalisches Praktikum PPBphys2

winter semester 2021/22

06. September 2021

EMMA RAULAND UND ANNA-LENA VESPER

advisor: Sanchayeeta Jana

Contents

1 Motivation	3
2 Background	4
2.1 Nuclear spin and quantum number of the rubidium isotopes	4
2.2 Important terms	5
2.3 Cross-Over Resonance	7
2.4 Two beam splitter cubes, $\lambda/2$ -plate and filter wheel in the experiment	8
2.5 Hyperfine structure constants and hyperfine transitions	8
3 Measurement protocol	10
3.1 Set up	10
3.2 Implementation	10
3.3 Measurements	11
3.4 Measuring instruments	11
4 Evaluation and discussion	12
4.1 Absorption spectrum and identification of lines	12
4.2 Calculation of the energy level distance of the absorption spectrum .	16
4.2.1 With current-wavelength characteristic	16
4.2.2 With the Fabry-Pérot interferometer	16
4.3 Ratio of the two rubidium isotopes	19
4.4 Dopplerfree signal	20
4.5 Hyperfine structure constant	25
4.6 Calculation of gas temperature/velocity for all temperatures	25
5 Summary	28
Bibliography	29
A Original protocol	30

1 Motivation

The hyperfine structure is the smallest energy distance of atoms known yet.

Among other things in the following experiment the hyperfine structure of rubidium is measured, by using Doppler free spectroscopy.

Rubidium can be handled as one electron system and alike hydrogen, which is useful for several calculations.

Furthermore the apportion spectrum is evaluated, the transition energies, the ratio of two isotopes ^{85}Rb and ^{87}Rb , the hyperfine structure constants and the gas temperature are calculated by using one experimental setup.

2 Background¹

2.1 Nuclear spin and quantum number of the rubidium isotopes

The spins of the protons and neutrons yield the nuclear spin. The number of neutrons of the rubidium isotopes differ, so their nuclear spin is different.

Rubidium 85 has an I of ²: $I = \frac{5}{2}$.

Rubidium 87 has an I of ³: $I = \frac{3}{2}$.

	$5^2S_{1/2}$	$5^2P_{1/2}$	$5^2P_{3/2}$
N	5	5	5
L	0	1	1
S	$\frac{1}{2}$	$\frac{1}{2}$	$\frac{1}{2}$
J	$\frac{1}{2}$	$\frac{1}{2}$	$\frac{3}{2}$

Table 2.1: quantum number of the rubidium isotopes for ground state and the first excited state

With $|i - j| \leq f \leq |i + j|$ following values for the both isotopes are produced:

F	$5^2S_{1/2}$	$5^2P_{1/2}$	$5^2P_{3/2}$
85-Rb	2;3	2;3	1;2;3;4
87-Rb	1;2	1;2	0;1;2;3

Table 2.2: F-quantum number of the rubidium isotopes for ground state and the first excited state

¹source: [Köh21]

²source: [Ste13], pp. 16

³source: [Ste15], pp. 16

2.2 Important terms⁴

Natural line width

The natural line width is the smallest possible width of a spectral line without external influence. Atoms have a finite radiation duration. The radiation of energy can be described as a damped harmonic oscillator. You get a vibration amplitude that decays over time with damping constant γ .

$$x(t) \approx x_0 \cdot e^{-(\frac{\gamma}{2})t} \cdot \cos(\omega_0 t)$$

You obtain the frequency spectrum $A(\omega)$ by Fourier transforming the vibration amplitude.

$$A(\omega) = \frac{x_0}{\sqrt{8\pi}} \left[\frac{1}{i(\omega_0 - \omega) + \frac{\gamma}{2}} + \frac{1}{i(\omega_0 + \omega) + \frac{\gamma}{2}} \right]$$

The spectral power density is $P_\omega \propto A(\omega) \cdot A^*(\omega)$ and has the shape of a Lorentz profile.

You receive the half width:

$$\delta\omega_n = \gamma \text{ und } \delta\nu_n = \frac{\gamma}{2\pi}$$

Another way to explain the natural line width is by using Heisenberg's uncertainty principle. The energy levels have an uncertainty of:

$$\Delta E \cdot \Delta t \leq \hbar$$

With the live time τ the energy uncertainty ΔE and the peak width at half height $\Delta\nu$ are following:

$$\Delta E = \frac{\hbar}{\tau}$$

$$\Delta\nu = \frac{\Delta E}{h} = \frac{1}{2\pi\tau}$$

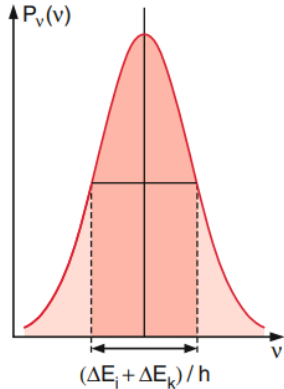


Figure 2.1: natural line width

⁴source: [Dem15], [Dem07a]

2 Background

Doppler broadening

Because of the Doppler effect the natural line width is increased, that's called Doppler broadening.

Different particles oscillate due to thermal movement relative to the observer and to one another thus causing the Doppler effect. The observer sees different frequencies. The profile of the Doppler-broadening spectral line is Gaussian distributed, while the profile of the natural line width is a Lorentz profile:

$$P(\omega) = P(\omega_0) \cdot e^{-[c \frac{\omega - \omega_0}{\omega_0 \cdot v_w}]^2}$$

The Doppler-broadening is bigger than the peak width at half-height of the natural line width:

$$\delta\omega_D = \frac{\omega_0}{c} \cdot \sqrt{\frac{8k_B T \cdot \ln(2)}{m}}$$

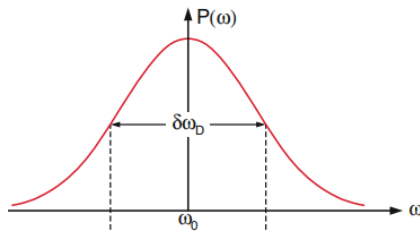


Figure 2.2: profile of a Doppler-broadening spectral line

The Doppler width increases with higher ω_0 and higher temperature and decreases with higher mass.

At atomic transitions the effect is so big, that the hyperfine structure can no longer be dissolved, without using a special experimental set-up.

Homogeneous/inhomogeneous expansion

You can distinguish between different mechanisms, which extend the natural line width with this method.

The probability of the emission, of a certain frequency ω is equal for all particles, with the homogenous expansion. With the inhomogeneous expansion that's not the case.

Saturation widening

Due to the high intensities a laser can reach, the pump beam can cause (wholly or partially) a saturation of the occupation densities, which leads to a broadening of the natural line width.

The saturation parameter S is defined by: $S(\omega) = S(\omega_0) \cdot \frac{(\gamma/2)^2}{(\omega - \omega_0)^2 + (\gamma/2)^2}$
 ω_0 stands for the resonance frequency of the regarded transition, whereas γ is the natural line width.

The absorption coefficient of the saturated transition is described by:

$$\alpha_s(\omega) = \alpha_0(\omega_0) \cdot \frac{(\gamma/2)^2}{(\omega - \omega_0)^2 + (\gamma_s/2)^2}$$

This is again a Lorentz profile (where $\alpha_0(\omega_0)$ describes the unsaturated absorption

coefficient (at resonance frequency)) with the broader line width
 $\gamma_s = \Delta\omega_s = \Delta\omega_0(1 + S_0)^{1/2}$

2.3 Cross-Over Resonance⁵

Cross-over resonance always occurs, when the frequency difference $\omega_2 - \omega_1$ for two transitions with frequencies ω_1 and ω_2 with the same upper or lower level is smaller than the Doppler width. In our experiment the transitions have the same lower level.

With a laser frequency $\omega_L = \frac{\omega_1 + \omega_2}{2}$ it is possible for the sample beam to saturate a velocity class $v_z dv_z = \frac{\omega_2 - \omega_1}{2k} \pm \frac{\gamma}{k}$ on the transition ω_1 and for the probe beam to saturate the velocity class $v_z dv_z = \frac{\omega_1 - \omega_2}{-2k}$ on the transition ω_2 .

Therefore, additionally to the direct resonances (at ω_1 and ω_2) a cross-over resonance is now visible in the spectrum. A cross-over resonance is the result of one beam causing a decrease of the occupation density of the shared lower level (respectively increase in the shared upper one) for molecules with a velocity class $v_z \neq 0$, with which the other beam can interact at the same time on another transition.

Since there are now more lines, the spectrum is more complex. But the advantage of the cross-over resonances is, that the energy distance of the levels that are both not the shard one is easily determined.

The cross-over resonances are usually the stronger signals because of the interaction of two velocity classes.

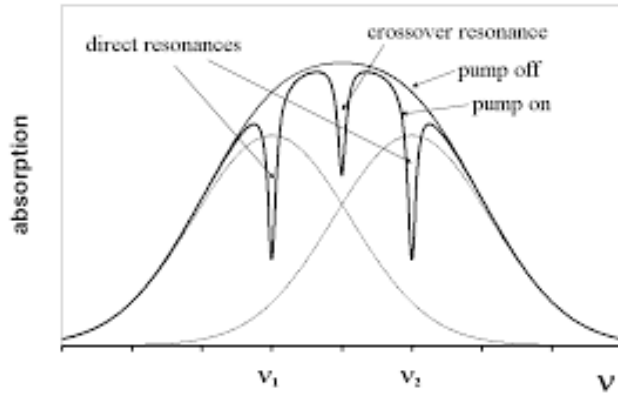


Figure 2.3: cross-over resonance⁶

⁵source: [Dem07b]

2 Background

2.4 Two beam splitter cubes, $\lambda/2$ -plate and filter wheel in the experiment

Two beam splitter cubes

The beam splitter cubes ist used to spilt light beams. It can be adjusted by blocking the Pump-beam.

$\lambda/2$ -plate and filter wheel

The $\lambda/2$ -plate is constructed by anisotropic crystals. The refractive index is dependent on the polarisation of the light. It is used to change the polarisation direction of linear polarised light. After the plate the polarisation is rotated by 2α .

In the experiment the $\lambda/2$ -plate is used to regulate the intensity. After the $\lambda/2$ -plate a beam splittter is being put. One polarisation direction can go through the other is being refelected.

with the filter wheel the intensities can be conformed.

2.5 Hyperfine structure constants and hyperfine transitions

Hyprefine structure contant⁷

In the experiment we will record an absorption spectrum of the hyperfine structure. Using the location of the absorption lines, it is possible to determine the necessary transition energy which equates to ΔE_{HFS} .

$$\Delta E_{HFS} = \frac{a}{2}[F(F+1) - J(J+1) - I(I+1)]$$

Since the quantum numbers are also known, the equation can be first reconfigured and then be solved for a.

Hyprefine transitions⁸

With the known selection rules $\Delta J = 0, \pm 1$, $\Delta I = 0, \pm 1$ and $\Delta F = 0, \pm 1$ the following transitions(marked in green) are possible:

⁷Source: [Köh21]

⁸Source: [Ste13],[Ste15]

2.5 Hyperfine structure constants and hyperfine transitions

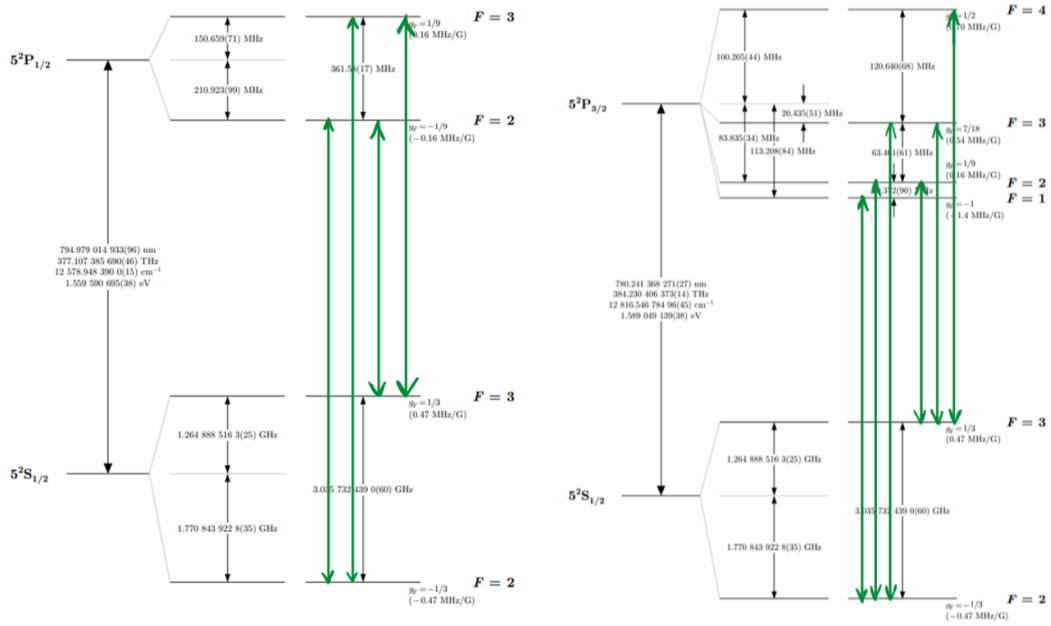


Figure 2.4: possible transitions for ^{85}Rb

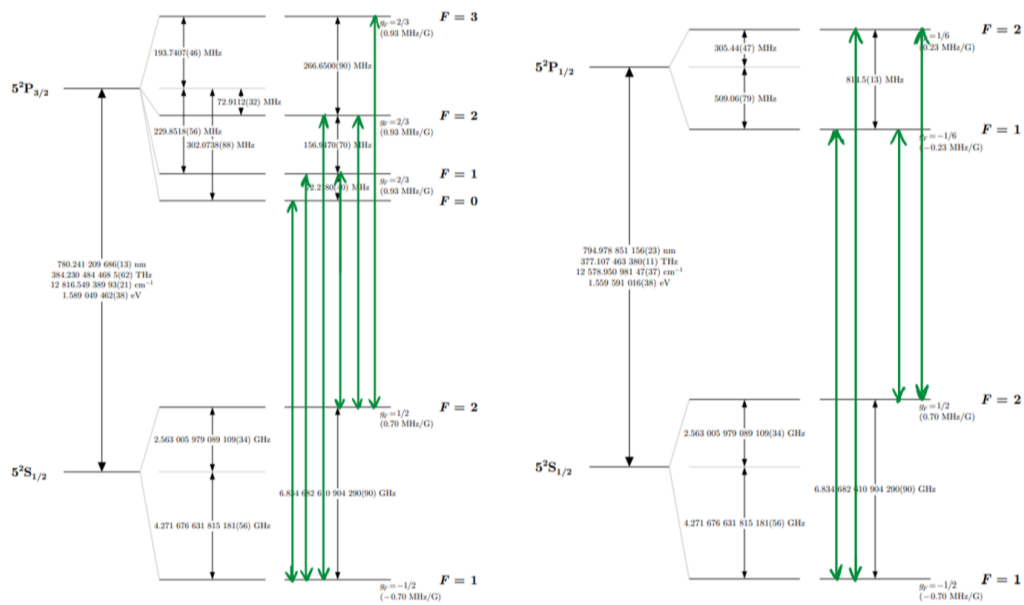


Figure 2.5: possible transitions for ^{87}Rb

3 Measurement protocol

3.1 Set up

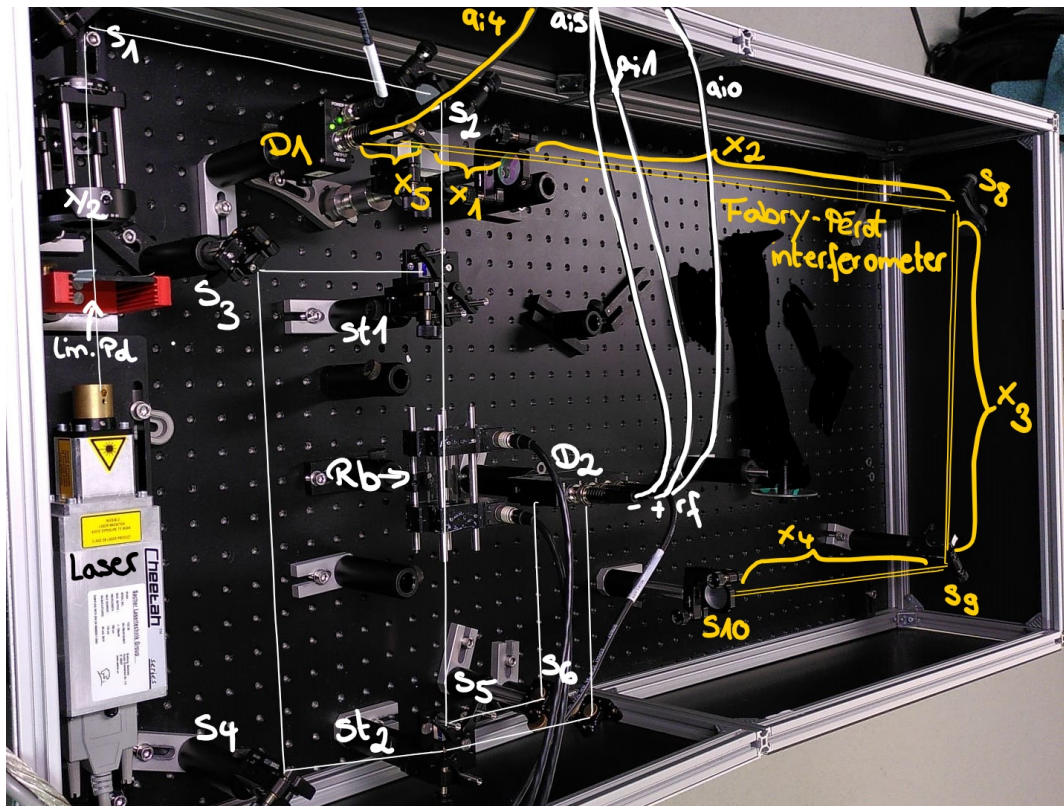


Figure 3.1: experimental setup

3.2 Implementation

The set up for the experiment was done according to the instruction and they mirrors were adjusted like described in the instruction and by our supervisor. The colors for the output in the measurement program are assigned as listed below:

ai0: white/black (reference output from D2)

3.3 Measurements

ai1: red (monitor + from D2)
ai3: blue (monitor - from D2)
ai4: yellow (D1)
(y-axis: amplitude in V; x-axis: laser current in mA)

The measurement data is saved under 06092021_time_group8.Rb87_xy_z (time stands for the exact time, when the data was taken, x,y and z are digits used to distinguish the different data sets)

3.3 Measurements

Main measurement

Table with information about the settings and how the data is stored: see appendix(A) page 2

Lengths for Fabry-Perot interferometer

$$\begin{aligned}x_1 &= (12.1 \pm 0.2) \text{ cm} \\x_2 &= (73.5 \pm 0.2) \text{ cm} \\x_3 &= (36.5 \pm 0.2) \text{ cm} \\x_4 &= (42.5 \pm 0.2) \text{ cm} \\x_5 &= (9.2 \pm 0.2) \text{ cm}\end{aligned}$$

Laser current - wavelength relation

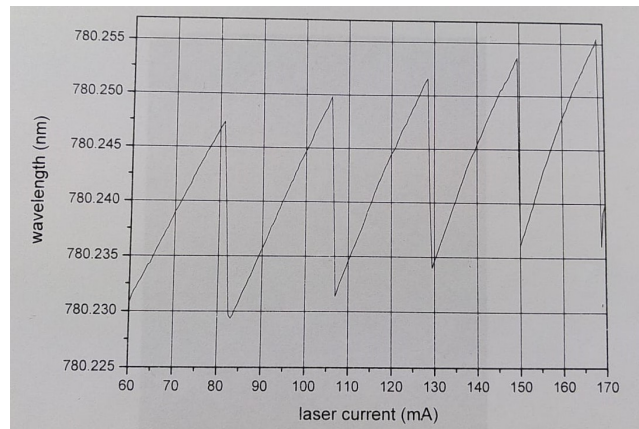


Figure 3.2: wavelength in nm as a function of the laser current in mA

3.4 Measuring instruments

List of the measuring instruments used: see appendix(A) page 3

4 Evaluation and discussion

4.1 Absorption spectrum and identification of lines

Task 1 to 5 are done with the measurements for 60°C because the lines are the most clear.

Detrending the data

First, the data needs to be freed from the trend.

Since it is pretty obvious, that the data has an increasing, linear trend, we used a python program to perform a linear regression to determine the trend, and then subtract that trend from our data.

In figure 4.1 this is done symbolic for the measurement of the full range.

All further data, that we use, will be trend freed the same way, but not explicitly shown again.

Identifying the lines

Since more exact measurements were done with a mode jump in between, the identification will be done with the data of our full scan range measurement, limited to an area from 115mA to 140mA because there is no mode jump in between. However, since we do have less data points, the results could be a bit vague.

To best determine the position of the peaks, we fitted all four peaks to a Gauss curve (figure 4.2) of the form:

$$y = a \cdot e^{-\frac{(x-x_0)^2}{2 \cdot \sigma^2}}$$

(again using a python program).

The exact position of the peak of the Gaussian fit can be obtained from the fitted parameters and are displayed at tabular 4.1, however they are rounded to three decimal digits because it is not possible to determine the wavelength according to the current from figure 3.2 as exact as the result of the fit.

The literature values can be determined with the help of the additional material¹. The mentioned F describes a transition with the lower level $5^2S_{1/2}F$.

¹[Ste13], [Ste15]

4.1 Absorption spectrum and identification of lines

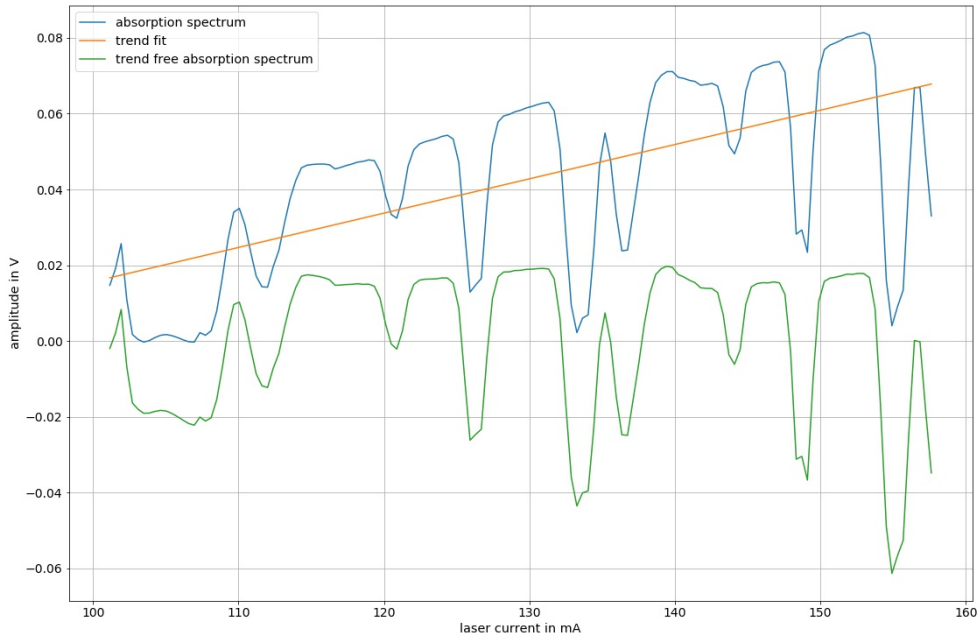


Figure 4.1: Detrending of the full scan range measurement

	I in [mA]	λ in [nm]	f in $[10^{14}Hz]$
1st dip	120.73	780.24500 ± 0.0005	3.8422862 ± 0.0000025
2nd dip	126.253	780.25000 ± 0.0005	3.8422616 ± 0.0000025
3rd dip	133.532	780.23875 ± 0.0005	3.8423170 ± 0.0000025
4th dip	136.604	780.24250 ± 0.0005	3.8422985 ± 0.0000025

Table 4.1: laser current, wavelength and frequency of the four dips

4 Evaluation and discussion

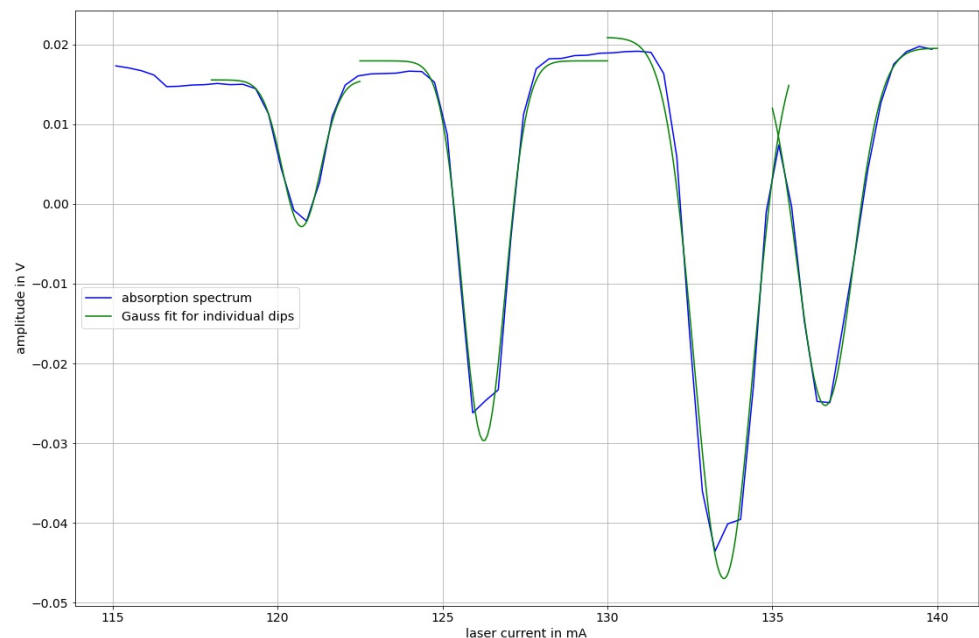


Figure 4.2: Fitting of the Gauss curve

4.1 Absorption spectrum and identification of lines

Line	Literature value
87-Rb,F=2	3.8422792
85-Rb,F=3	3.8422914
85-Rb,F=2	3.8423218
87-Rb,F=1	3.8423476

Table 4.2: Literature values of frequency for transitions

Within the error range, our values do not match with the literature values. With a bigger range, the first dip could be identified as $^{85}Rb, F=3$, the second dip would be $^{87}Rb, F=2$ and the third one $^{85}Rb, F=2$

However, the fourth dip does not in the slightest represent $^{87}Rb, F=1$.

Since these four peaks are between two mode jumps, we would suspect to see an steady increase of the wavelength of these peaks(from left to right). But in the given graph with the laser current and wavelength(figure 3.2) there appears to be a mode jump around 130 mA, which does not exist in our measurement.

For the following tasks, we therefore identify the lines not using (figure 3.2), but according to their literature values from highest frequency (lowest wavelength) all to the left to lowest frequency (highest wavelength) all to the right (because like said before, we would expect to see the wavelength of the peaks increase from left to right).

So from left to right the first dip is $^{87}Rb, F = 1$, the second one $^{85}Rb, F = 2$, the third one $^{85}Rb, F = 3$ and the fourth one $^{87}Rb, F = 2$.

We are also going to use our initial data going forward because we have more values for these, which is crucial for some parts of our evaluation.

Therefore the order of the dips changes like this:

From left to right: 1st $^{85}Rb, F = 3$, 2nd $^{87}Rb, F = 2$, 3rd $^{85}Rb, F = 3$ and fourth $^{87}Rb, F = 2$.

4 Evaluation and discussion

4.2 Calculation of the energy level distance of the absorption spectrum

4.2.1 With current-wavelength characteristic

For the calculation of the energy level distance of the absorption spectrum with the current-wavelength characteristic figure 3.2 and figure 4.3 are used.

You read in figure 4.3 at which current the dips of the absorption spectrum (blue graph and green line) lie. After that you determine the corresponding wavelength λ_i in figure 4.4.

The energy can be calculated with:

$$E_i = \frac{hc}{\lambda_i}$$

The corresponding error is:

$$s_{E_i} = \frac{hc}{\lambda_i^2} \cdot s_{\lambda_i}$$

The energy level distance is:

$$\Delta E_{i,i+1} = E_i - E_{i+1}$$

The error of $\Delta E_{i,i+1}$ is:

$$s_{\Delta E_{i,i+1}} = \sqrt{(s_{E_i})^2 + (-s_{E_{i+1}})^2}$$

	I in [mA]	λ in [nm]	E in $[10^{-24} J]$	$\Delta E_{i,i+1}$ in $[10^{-24} J]$
1st dip	132.3 ± 0.2	780.2363 ± 0.0005	$254600.41 \pm 0, 16$	1.40 ± 0.23
2nd dip	135.2 ± 0.2	780.2406 ± 0.0005	$254599.00 \pm 0, 16$	2.32 ± 0.23
3rd dip	142.3 ± 0.2	780.2477 ± 0.0005	$254596.69 \pm 0, 16$	1.24 ± 0.23
4th dip	147.3 ± 0.2	780.2515 ± 0.0005	$254595.45 \pm 0, 16$	

Table 4.3: laser current, wavelength and energy of the four dips

4.2.2 With the Fabry-Pérot interferometer

The free spectral range of the Fabry-Pérot interferometer is given by:

$$\Delta\nu_{FSR} = \frac{c}{2nd}$$

Here $n = 1$, because the medium is air and $d = x_3 + x_4 = 42.5cm + 36.5cm = 79.0cm = 0.790m$.

$$\Delta\nu_{FSR} = \frac{c}{2d} = \frac{c}{1.58m} = 189742062Hz$$

The errors s_d and $s_{\Delta\nu_{FSR}}$ follow with the law of error propagation:

$$s_d = \sqrt{(\frac{\partial d}{\partial x_3} \cdot s_{x_3})^2 + (\frac{\partial d}{\partial x_4} \cdot s_{x_4})^2} = \sqrt{0.000008m^2} = 0.002828427m \approx 0.003m$$

$$s_{\Delta\nu_{FSR}} = \sqrt{(\frac{\partial \Delta\nu_{FSR}}{\partial d} \cdot s_d)^2} = \frac{c}{2d^2} \cdot s_d = 679331.1328Hz$$

4.2 Calculation of the energy level distance of the absorption spectrum

$$\Delta\nu_{FSR} = \underline{(189.7 \pm 0.7) \cdot 10^6 Hz}$$

By counting the number of dips of the Fabry-Pérot interferometer (green graph) (see figure 4.3) in a certain range and taking the mean, the frequency axis (purple) can be created and scaled. Using this axis one can find the number of frequency steps (n_d) in units of $\Delta\nu_{FSR}$, that lie between two dips. The dips are marked with a green line.

The energy level distance follows as:

$$\Delta E = n_d \cdot h \cdot \Delta\nu_{FSR}$$

The error can be calculated with:

$$s_{\Delta E} = h \cdot \sqrt{(\Delta\nu_{FSR} \cdot s_{n_d})^2 + (n_d \cdot s_{\Delta\nu_{FSR}})^2}$$

distance between	n_d	ΔE in $[10^{-24} J]$
1st and 2nd dip	13 ± 1	1.63 ± 0.13
2nd and 3rd dip	32 ± 1	4.02 ± 0.13
3rd and 4th dip	23 ± 1	2.89 ± 0.13

Table 4.4: energy level distance between the dips

Comparison of the two methods

Both methods of calculating the energy level distance lead to results, that are similar in their scale (see table 4.4 and table 4.3).

In the case of errors only the energy level distance between the 1st and 2nd dip correspond. The other results differ stronger.

This might be the case because especially the first method is not very precise. Here the wavelength was determined by a photographed picture. For a better result more and better data of the wavelength- laser current function would be help full.

Another reason for this discrepancy is, the in section 4.1 explained measurement between two mode jumps. This may lead to a slightly wrong $\Delta\nu_{FSR}$.

4 Evaluation and discussion

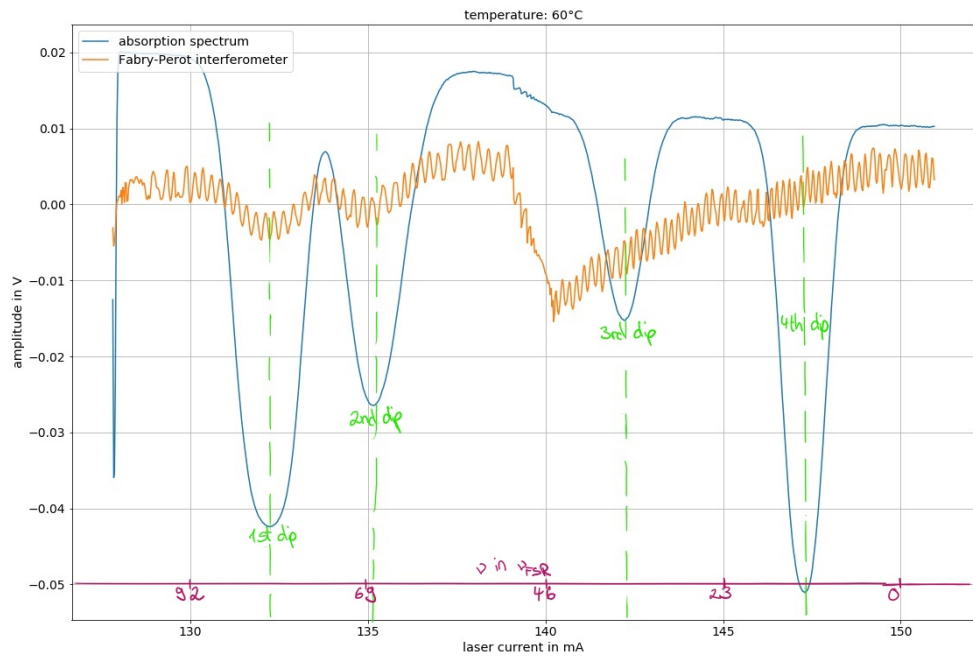


Figure 4.3: Trend free absorption spectrum; Fabry-Pérot interferometer

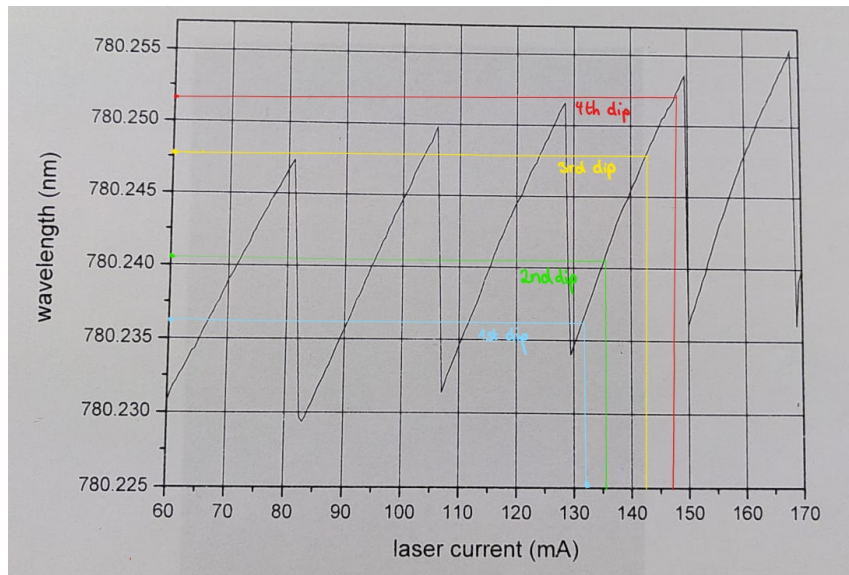


Figure 4.4: determination of the corresponding wavelength for 4.2.1 for 60°

4.3 Ratio of the two rubidium isotopes

For calculating the ratio of the rubidium isotopes, four Gaussian curves are fitted, with python, into the absorption spectrum (see figure 4.5). The green functions correspond to ^{85}Rb and the orange to ^{87}Rb .

The Gaussian function for this plot in general is:

$$f(x) = -a \cdot e^{\frac{-(x-x_0)^2}{2\cdot\sigma^2}} + y$$

parameters	a in $[10^{-2}\text{V}]$	x_0 in $[10^2\text{mA}]$	σ in $[10^{-1}\text{mA}]$	y in $[10^{-2}\text{V}]$
1st dip (^{87}Rb)	7.16659381	1.32234133	9.27443670	2.60286131
2nd dip (^{85}Rb)	4.05172184e	1.35173626	7.17072297	1.33127844
3rd dip (^{85}Rb)	2.75740134	1.42200564	5.68795384	1.20580887
4th dip (^{87}Rb)	6.62275898	1.47283901	5.68196043	1.30401357

Table 4.5: Gaussian functions for the dips

The integral is calculated as following:

$$\int_{-\infty}^{\infty} f(x)dx = \int_{-\infty}^{\infty} ae^{\frac{-(x-x_0)^2}{2\cdot\sigma^2}} dx = a\sqrt{2\pi\sigma^2}$$

This yields:

	$\int_{-\infty}^{\infty} f(x)dx$ in $[10^{14}]$
1st dip (^{85}Rb)	16.7
2nd dip (^{87}Rb)	7.28
3rd dip (^{87}Rb)	3.93
4th dip (^{85}Rb)	9.43

Table 4.6: Gaussian integral for the four dips

Both integrals for ^{87}Rb and ^{85}Rb are summed. From it results the ratio:

	calculated	literature ²
percentage of ^{85}Rb	69,9%	72,168%
percentage of ^{87}Rb	30,1%	27,835%

Table 4.7: percentage of ^{85}Rb and ^{87}Rb

²source: [unk53]

4 Evaluation and discussion

It can be said, that the calculated ratio of ^{85}Rb and ^{87}Rb is pretty close to the literature ratio. The value differs less than 3%. This shows, that the used method is suitable for calculating the ratio of the different isotopes.

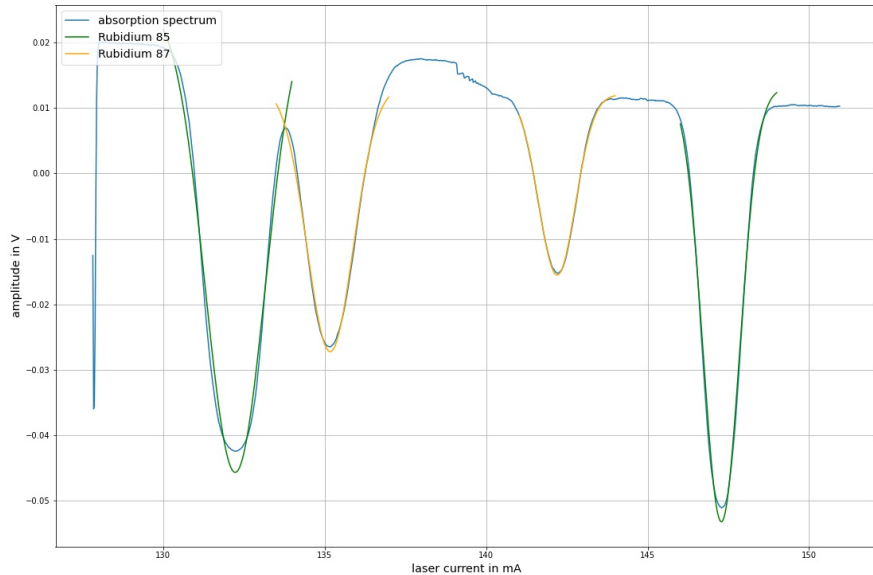


Figure 4.5: Gaussian curves fitted into the absorption spectrum

4.4 Dopplerfree signal

The Doppler free absorption spectrum of all dips are plotted individually with python. You can see the hyperfine structure of each dip.

4.4 Dopplerfree signal

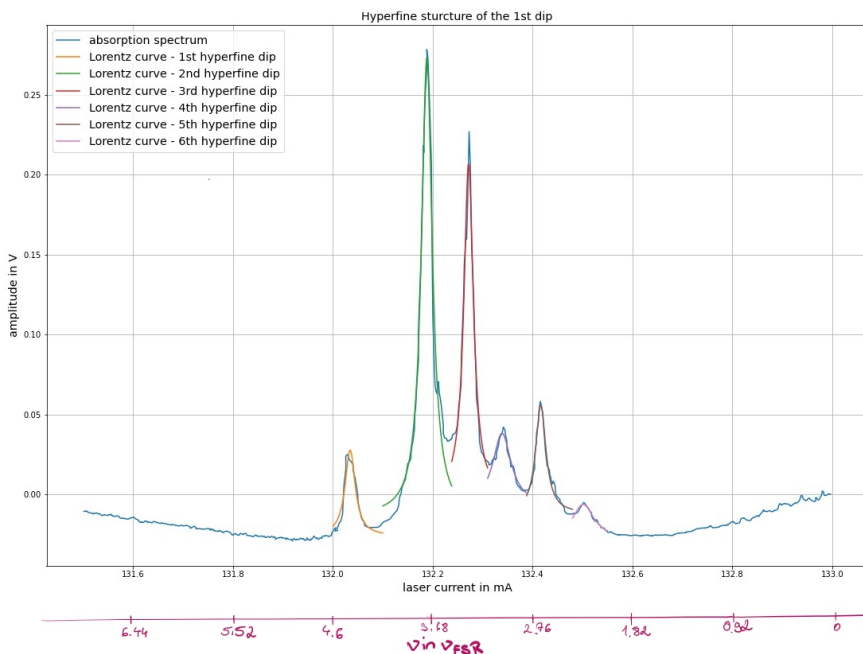


Figure 4.6: Doppler free signal of the 1st absorption dip with fitted Lorentz curves

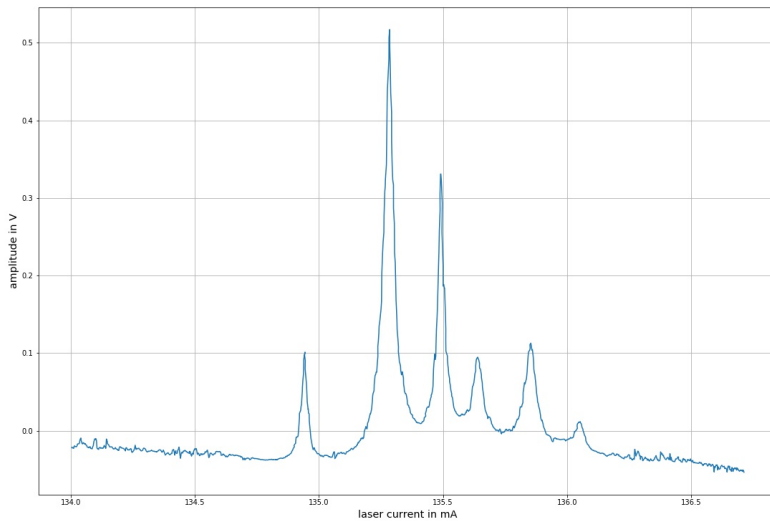


Figure 4.7: Doppler free signal of the 2nd absorption dip

4 Evaluation and discussion

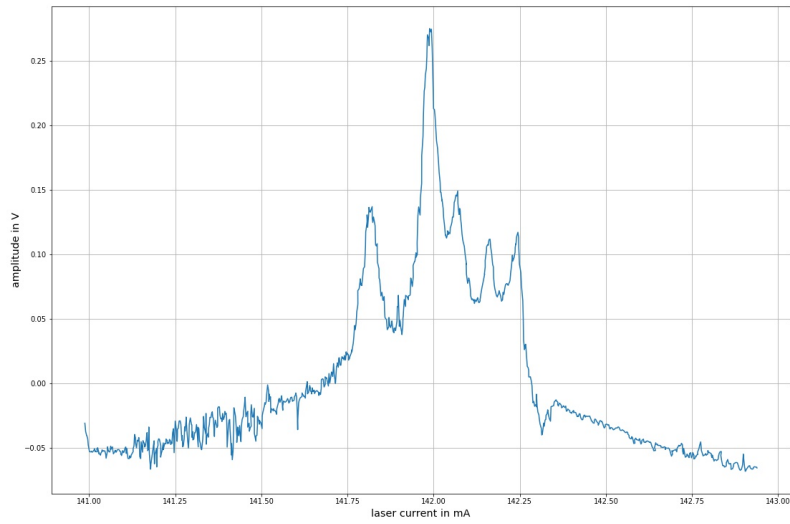


Figure 4.8: Doppler free signal of the 3rd absorption dip

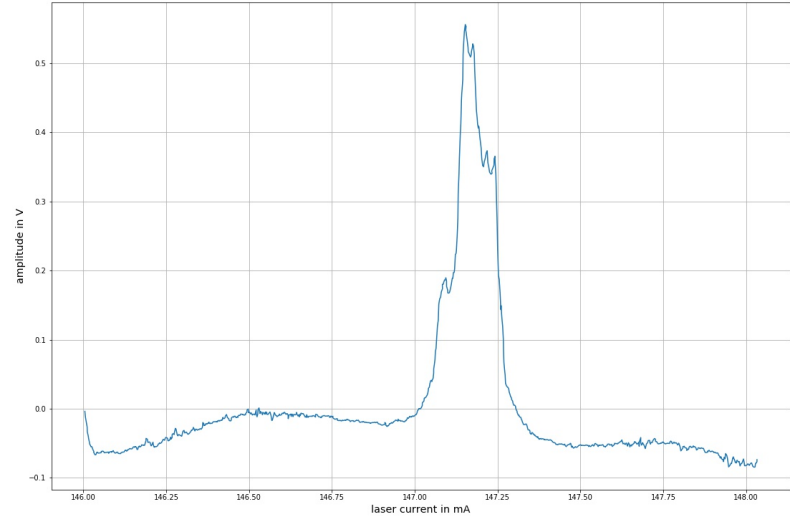


Figure 4.9: Doppler free signal of the 4th absorption dip

4.4 Dopplerfree signal

The hyperfine structure of each dips is different, only dip one and two look similar. They all have smaler and taller hyperfine dips. The taller ones are more likely to be cross over signals (see section 2.3).

In the following part the first dip (figure 4.6) is examined more precisely.

Here the Lorentz curves are fitted to the individual hyperfine dips with the formula:

$$f(x) = y + \frac{2a}{\pi} \cdot \frac{w}{4 \cdot (x - x_0)^2 + w^2}$$

Where a is the amplitude, w the width and x_0 is the position.

You can convert the positions from mA into J by using figure 4.4 and the formula $E = h \cdot \nu = \frac{hc}{\lambda}$.

To determine the distance of the hyperfine dips you use ν_{FSR} from section 4.2.2. A new frequency axis, with chosen zero position, is fitted into the plot.

	position in mA	E_i in $10^{-26}J$
1st hyperfine dip	132.034615	25460036.8
2nd hyperfine dip	132.188304	25460038.7
3rd hyperfine dip	132.271937	25460041.0
4th hyperfine dip	132.338760	25460042.8
5th hyperfine dip	132.416446	25460043.1
6th hyperfine dip	132.501397	25460043.5

Table 4.8: positions of the hyperfine dips of the 1st dip

	$\Delta E_{i,i+1}$ in $10^{-26}J$	$\Delta \nu_{i,i+1}$ in MHz
1st hyperfine dip	4.24	64.0
2nd hyperfine dip	2.33	35.1
3rd hyperfine dip	1.78	26.8
4th hyperfine dip	2.05	31.0
5th hyperfine dip	2.46	37.2
6th hyperfine dip		

Table 4.9: distances of the hyperfine dips of the 1st dip

4 Evaluation and discussion

In section 4.1 it was determined, that the dip belongs to ^{85}Rb $F = 3$. Therefore the dip has three different hyperfine dips (see figure 2.4). The hyperfine dips are assigned as following:

1st hyperfine dip: $F = 4 \rightarrow F = 3$

2nd hyperfine dip: crossover resonanz between 1st and 4th dip

3rd hyperfine dip: crossover between 1st and 6th dip

4th hyperfine dip: $F = 3 \rightarrow F = 3$

5th hyperfine dip: crossover between 4st and 6th dip

6th hyperfine dip: $F = 2 \rightarrow F = 3$

The crossover resonance dips are taller, than the other ones (see section 2.3), which explains the height of dip 2, 3 and 5.

F	$\Delta\nu_{measured}$ in MHz	$\Delta\nu_{literature}$ ³ in MHz
$4 \iff 3$	125.9	120.640
$3 \iff 2$	68.2	63.401

Table 4.10: frequency distances of the transition

The measured frequency distance compared to the literary value differs by $5MHz$. One reason for this difference might be the $\Delta\nu_{FSR}$. Like in section 4.2 explained it was determined using two different mode jumps. Nevertheless it can be said that the transitions are assigned correct, because the scale is right and the value of other transitions would differ much stronger.

³source [Ste13], pp. 25

4.5 Hyperfine structure constant

The hyperfine structure constant (a) is calculated by using:

$$a = \frac{2 \cdot \Delta E_{hfs}}{F(F+1) - I(I+1) - J(J+1)}$$

ΔE_{hfs} is the distance between the hyperfine dips (ΔE_i) and the normal state (ΔE_g). For one transition the quantum numbers I and J stay the same. You get:

$$a = \frac{2 \cdot (\Delta E_i - \Delta E_g)}{F_1(F_1+1) - F_2(F_1+2)} = \frac{2h \cdot (\Delta \nu_i - \Delta \nu_g)}{F_1(F_1+1) - F_2(F_1+2)}$$

The literature values of a are calculated the same way as the measured values just with $\Delta \nu_i - \Delta \nu_g$ from source [Ste13], pp.25.

The measured values of $\Delta E_i - \Delta E_g$ are from section 4.4. So a is intended for the same transitions of ^{85}Rb ($F = 4 \rightarrow F = 3$; $F = 3 \rightarrow F = 2$; $F = 2 \rightarrow F = 3$).

F	$a_{measured}$ in $10^{-26}J$	$a_{literature}^4$ in $10^{-26}J$
$4 \iff 3$	2.086	1.332
$3 \iff 2$	1.506	1.400

Table 4.11: For the transitions of ^{85}Rb calculated and literature hyperfine constant

The calculated a is in the same scale as the literature value. Conspicuous is, that the first measured value is twice as high as the literature value. The other value fits quite nice.

4.6 Calculation of gas temperature/velocity for all temperatures

For this task we fit a Gauss curve to the absorption dip $^{85}Rb, F = 3$ for all three temperatures (like it was done in task 1 4.1)

σ relates to the full width at half maximum like this:

$$fwhm = 2\sqrt{2 \cdot \ln(2)} \cdot \sigma$$

From 2.2 we know, that the Doppler width (full width at half maximum) is defined as:

$$\delta\omega_D = \frac{\omega_0}{c} \cdot \sqrt{\frac{8k_B T \cdot \ln(2)}{m}}$$

With the fitted parameters from our Gauss curve and these two formulas, we can now determine the temperature of the gas.

With the Maxwell-Boltzmann distribution (and the temperatures) we can then also calculate the most likely velocity and the average velocity as follows:

⁴source [Ste13], pp. 25

4 Evaluation and discussion

$$v_w = \sqrt{\frac{2k_B T}{m}}$$

$$\bar{v} = \sqrt{\frac{8k_B T}{\pi \cdot m}}$$

As "literature" values for the velocities we put the temperatures that we read from the heater into the two formulas above.

To get σ in Hz instead of mA we use our result from 4.2:

$$\sigma[\text{Hz}] = \sigma[\text{mA}] \cdot \Delta\nu_{fsr} \cdot \frac{23}{5}$$

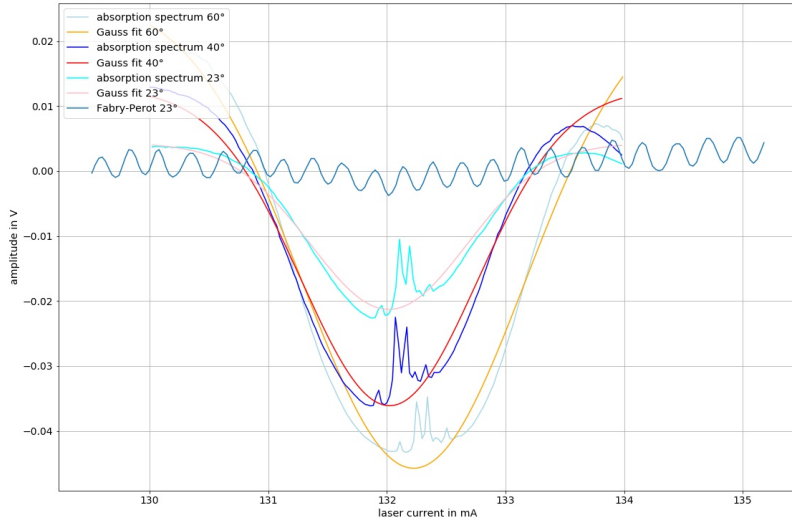


Figure 4.10: 1st absorption dip for all temperatures with fitted Gauss curve

$T_{theo}[K]$	$fwhm[GHz]$	$T_{calc}[K]$	$v_w[m/s]$	$v_{w,\text{theo}}[m/s]$	$\bar{v}[m/s]$	$\bar{v}_{\text{theo}}[m/s]$
296.15	1.25937	1778.203	590.118	240.826	665.877	271.743
313.15	1.46534	2407.404	686.630	247.642	774.779	279.434
329.25	1.90577	4072.048	893.007	253.928	1007.650	286.527

Table 4.12: Temperature and velocities for all temperatures

As can be seen in table 4.12, our calculated temperatures and therefore also the velocities, are way too high (the temperature values are almost of a factor 10 too big). One possible explanation for this could be, that we have another mechanism, that widens the natural line width, that we don't know of.

4.6 Calculation of gas temperature/velocity for all temperatures

By comparing the absorption spectrum for the different temperature values it is visible, that with increasing temperature the absorption line broadens and gets bigger (higher amplitude).

5 Summary

Summarised can be said, that the used methods led to mostly unsatisfactory results. The whole evaluation was a bit frustrating because we were not quite sure, if we made a mistake during the measurement or if something with our data is not right.

Nevertheless, this experiment was good for getting a better overview of lecture for atoms and nuclear. We got to know how to (theoretically) measure and evaluate the absorption spectrum and even the hyperfine structure of rubidium. Its fascinating seeing the theoretically learned formulas and knowledge in a practical way.

Bibliography

- [Dem07a] Wolfgang Demtröder. Laserspektroskopie - Grundlagen und Techniken. 5. Auflage. Berlin, Heidelberg: Springer-Verlag, 2007, pp. 55–62.
- [Dem07b] Wolfgang Demtröder. Laserspektroskopie - Grundlagen und Techniken. 5. Auflage. Berlin, Heidelberg: Springer-Verlag, 2007, pp. 317–318.
- [Dem15] Wolfgang Demtröder. Experimentalphysik 3 - Atome, Moleküle und Festkörper. 5. Auflage. Berlin, Heidelberg: Springer-Verlag, 2015, pp. 227–230.
- [Köh21] Prof. Dr. Jürgen Köhler. script for the lecture EPB2. University of Bayreuth, 2021.
- [Ste13] Daniel Adam Steck. Rubidium 85 D Line Data. revision 2.1.6. 1274 University of Oregon: Oregon Center for Optics and Department of Physics, 20 September 2013. URL: <http://steck.us/alkalidata>.
- [Ste15] Daniel Adam Steck. Rubidium 87 D Line Data. revision 2.1.5. 1274 University of Oregon: Oregon Center for Optics and Department of Physics, 13 January 2015. URL: <http://steck.us/alkalidata>.
- [unk08] unknown. Saturated Absorption Spectroscopy. University of Florida, March 4 2008, p. 10. URL: https://www.institut3b.physik.rwth-aachen.de/global/show_document.asp?id=aaaaaaaaajwfgs.
- [unk53] unknown. Rubidium. latest edit: 20.05.2021, 01:53. URL: <https://de.wikipedia.org/wiki/Rubidium>.

A Original protocol

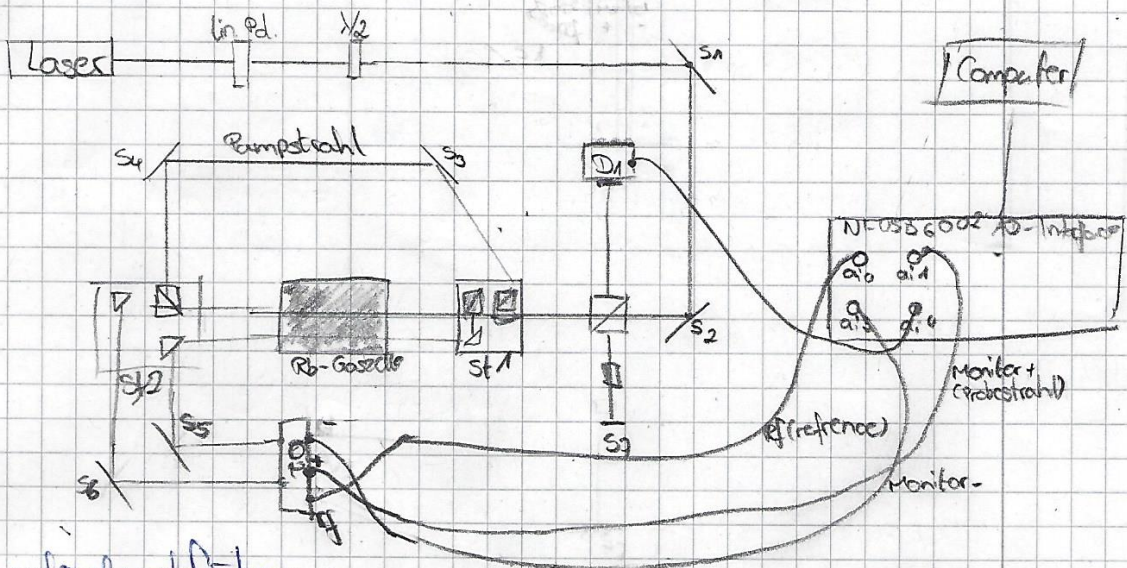
Versuch Spektroskopie an Rubidiumgas

Teilnehmer: Emma Rawland und Anna-Lena Vesper

Datum: 06. September 2021

Raum: 3.O.Og BGU

Versuchsaufbau:



Versuchsdurchführung:

Der Versuchsaufbau wird, wie im Skript beschrieben realisiert und die Spiegel werden dementsprechend justiert.

Im Messprogramm haben die Ausgänge folgende Farben,

a_{i0} : weiß/schwarz (rf an D_2)

a_{i1} : rot (Monitor + an D_2)

a_{i3} : blau (Monitor - an D_2)

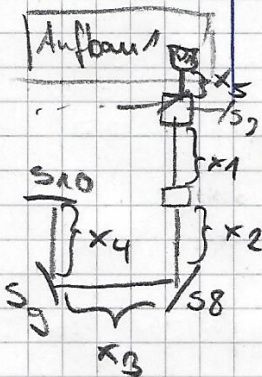
a_{i4} : gelb (D_1) Interferometer

(Amplitude in V - y-Achse; Laserspannung in mV - x-Achse)

Die Messdaten sind unter 06.09.2021_Uhrzeit_group8_Rb87_xy.z gespeichert.

Messtabellen - Die Daten werden mit der Ablenkung - Ky - z
gekennzeichnet wobei z für die Teilaufgabe und y für die Gasstrahl
stellt. z steht für je eine Einzellinie

Gas Temp / °C	Teilaufgabe	Laser		Einstellungen		
		Current [mA]	Temp [°C]	dt/pixel	Vscan step's	Ablenkung
$23,0 \pm 0,1$	1	140,0	220,0	150	1000	-123
	2.1 (single line)	132,0	-" -	150	1500	-223_1
	2.2 (double lines)	136,0 135,0	-" -	150	1500	-223_2
	2.3 (double lines)	143,0	-" -	-"	-4-	-223_3
	2.4 (double lines)	147,5	-" -	-4-	-4-	-223_4
$40,0 \pm 0,1$ (normal)	1	140,0	-" -	-" -	1000	-140
	2.1	133,0	-" -	-" -	1500	-240_1
	2.2	136,0	-" -	-" -	-" -	-240_2
	2.3	143,0	-" -	-" -	-" -	-240_3
	2.4	147,5	-" -	-" -	-" -	-240_4
56,1 $56,1 \pm 0,1$ (normal)	1	140,0	-" -	-" -	1000	-2160
	2.1	133,0	-" -	-" -	1500	-260_1
	2.2	136,0	-" -	-" -	-" -	-260_2
	2.3	143,0	-" -	-" -	-" -	-260_3
	2.4	147,5 142,5 148,0	-" -	-" -	-" -	-260_4



$$\begin{aligned}
 x_1 &: 12,1\text{ cm} \pm 0,2 \\
 x_2 &: 73,5\text{ cm} \pm 0,2 \\
 x_3 &: 36,5\text{ cm} \pm 0,2 \\
 x_4 &: 42,5\text{ cm} \pm 0,2 \\
 x_5 &: 9,2\text{ cm} \pm 0,2
 \end{aligned}$$

Messgeräte

Schraubfisch: THORLABS

Inventarnummer: 101273

Computer: Fujitsu

Inventarnr.: 91367

Bildschirm: LG

Inventarnr.: 91356

Interloch: LSU-ELU3 3117014

AD-Interface: NI-USB 6002 / 16 Bit 50 ns/s

Laser-Diode-Controller: PILOTpc 500 | Inventarnr.: 97423

Ablesefehler: $s_a = 0,05 \text{ mA}$

Temperatur controller: THORLABS; TC200

Inventarnr.: 97297

Ablesefehler: $0,1^\circ\text{C}$

Laser: Cheetah

Seriennr.: NC - 780 - 0716 - 0071

Detektor (D2): THORLABS - Balanced amplified photodetectors

Seriennr.: MO0335G22

Detektor (D1): THORLABS - PDA 100A-EC

Messband: HOLEX

Ablesefehler: 0,2 cm

Restfehler:

Unterschriften

1. Mesper